Confined Polymer Dynamics on Clay Platelets

ARTICLE *in* LANGMUIR · OCTOBER 2010

Impact Factor: 4.46 · DOI: 10.1021/la102667k · Source: PubMed

4 AUTHORS, INCLUDING:

Martin Brodeck
Forschungszentrum Jülich
11 PUBLICATIONS **124** CITATIONS
SEE PROFILE

Olaf Holderer
Forschungszentrum Jülich
62 PUBLICATIONS **536** CITATIONS
SEE PROFILE

H. Frielinghaus
Forschungszentrum Jülich
137 PUBLICATIONS **1,422** CITATIONS
SEE PROFILE

Langmuir
Article
pubs.acs.org/Langmuir

Confined Polymer Dynamics on Clay Platelets

Xiuli Frielinghaus,[†] Martin Brodeck,[†] Olaf Holderer,[‡] and Henrich Frielinghaus*[,‡]

[†]*Institute of Solid State Research, Forschungszentrum Jülich GmbH, 52425 Jülich, Germany, and* [‡]*Jülich Centre for Neutron Science, Forschungszentrum Jülich GmbH, Lichtenbergstrasse 1, 85747 Garching, Germany*

Received July 2, 2010. Revised Manuscript Received August 26, 2010

The structure and dynamics of poly(ethylene oxide) adsorbed on dispersed clay platelets are investigated by small-angle neutron scattering and neutron spin-echo spectroscopy. The intermediate scattering function has a mobile contribution described by the Zimm theory and an immobile contribution that is constant within the time window. The immobile fraction as a function of the scattering vector Q is described by a Lorentz function, from which a localization length is determined. The relaxation rates grow with polymer concentration in agreement with dielectric measurements but contrary to pure polymer gels.

Nanocomposites consisting of clay and polymer are produced by different methods,[1] depending on the desired raw materials. Different degrees of dispersion are known, ranging from stack dispersion over intercalation to full exfoliation. Usually, the most homogeneous state is preferred for the application. One very successful path for natural clays and poly(ethylene oxide) is intercalation from solution. Here, the two components are dissolved in water independently, and then the solutions are mixed and dried at low pressure and/or elevated temperature. Thus, the states after mixing during concentration are of principal interest. One structure at medium concentration was identified to be bicontinuous by the clay platelets, and the polymer decorates and interconnects the thin sheets.[2] First, dynamic measurements of polymer-decorated colloids have been performed. For instance, a polymer brush on spherical particles[3] influences the diffusion properties of the colloids in the concentrated region depending on the molar mass of the polymer because the interaction range of the effective potential varies. The mesoscopic movements of polymer-decorated clays were found to slow down with aging time as a result of gel formation.[4] Gelation can be controlled by the solvent quality.[5] In a complementary manner, microscopic movements of water in clay stacks are described by translations and rotations.[6] The 2D and 3D diffusion of water was distinguished.[7] In parallel, this was observed for tightly bound polymers.[8] Polymer dynamics in clay suspensions have been addressed by dielectric relaxation spectroscopy.[9,10] The relaxation times lie in the 20 ns range at room temperature.[9] With increasing polymer concentration, the relaxations become faster. This is in qualitative agreement with sound velocities[11] but opposes pure polymer gels.[12,13] The connection of a constraint region near the clay particles and the overall dynamics observed by rheological experiments was proposed in ref 14.

This article focuses on the dynamics of polymers adsorbed on clay platelets. The characterization was done by neutron spin-echo spectroscopy. The polymers are pointwise adsorbed onto the clay, and the resulting loops show confined Zimm-like movements. The relaxation curves were interpreted to result from an immobile and a mobile contribution. This leads us to the definition of a localization length (i.e., a polymer film thickness defined by the dynamic behavior but not seen in the static small-angle neutron-scattering measurements).

The Laponite clay for research and development (LRD) was kindly provided by Rockwood Clay Additives GmbH, Moosburg, Germany. The producer provided the dimensions of the clay particles with a diameter of $D = 200$ Å and a thickness of $d = 10$ Å. Poly(ethylene oxide) (PEO) with a molar mass of 20 kg/mol was obtained from Sigma-Aldrich (St. Louis, MO). The polydispersity M_w/M_n is better than 1.05. Heavy water with a degree of deuteration of 99.8% was purchased from Chemotrade (Leipzig, Germany). All materials were used as obtained without further purification. Two 1% stock solutions of LRD and PEO in D_2O were prepared. After being mixed, the solution was concentrated to 6% LRD using a rotovap.

Small-angle neutron-scattering experiments have been performed at the KWS-2 instrument at the FRM II research reactor. The neutron wavelengths were 7 and 20 Å, and the detector distances were 2 and 8 m. The samples were placed in quartz cells with an optical path length of 1 mm. The experiments took place at room temperature. For background correction, a D_2O-filled cell and a boron measurement were taken into account.

*Corresponding author. Tel: +49 89 289 10706. Fax: +49 89 289 10799. E-mail: h.frielinghaus@fz-juelich.de.

(1) Nguyen, Q. T.; Baird, D. G. *Adv. Polym. Technol.* **2006**, *25*, 270.
(2) Osaka, N.; Endo, H.; Nishida, T.; Suzuki, T.; Li, H. J.; Haraguchi, K.; Shibayama, M. *Phys. Rev. E* **2009**, *79*, 060801.
(3) Voudouris, P.; Choi, J.; Dong, H.; Bockstaller, M. R.; Matyjaszewski, K.; Fytas, G. *Macromolecules* **2009**, *42*, 2721.
(4) Zulian, L.; Ruzicka, B.; Ruocco, G. *Philos. Mag.* **2008**, *88*, 4213.
(5) Anyfantakis, M.; Bourlinos, A.; Vlassopoulos, D.; Fytas, G.; Ginnelis, E.; Kumar, S. K. *Soft Matter* **2009**, *5*, 4256.
(6) Bordallo, H. N.; Aldridge, L. P.; Churchman, G. J.; Gates, W. P.; Telling, M. T. F.; Kiefer, K.; Fouquet, P.; Seydel, T.; Kimber, S. A. J. *J. Phys. Chem. C* **2008**, *112*, 13982.
(7) Malikova, N.; Longeville, S.; Zanotti, J. M.; Dubois, E.; Marry, V.; Turq, P.; Ollivier, J. *Phys. Rev. Lett.* **2008**, *101*, 265901.
(8) Bae, S. C.; Granick, S. *Annu. Rev. Phys. Chem.* **2007**, *58*, 353.
(9) Sengwa, R.J.; Sankhla, S.; Choudhary, S. *Colloid Polym. Sci.* **2009**, *287*, 1013 and related work by same authors.
(10) Floudas, G.; Paraskeva, S.; Hadjichristidis, N.; Fytas, G.; Chu, B.; Semenov, A. N. *J. Chem. Phys.* **1997**, *107*, 5502.
(11) Bot, A.; Schram, R. P. C.; Wegdam, G. H. *Colloid Polym. Sci.* **1995**, *273*, 252.
(12) Kanaya, T.; Takahashi, N.; Nishida, K.; Seto, H.; Nagao, M.; Takeba, Y. *Physica B* **2006**, *385*−*386*, 676.
(13) Biehl, R.; Guo, X.; Prud'homme, R. K.; Monkenbusch, M.; Allgaier, J.; Richter, D. *Physica B* **2004**, *350*, 76.
(14) Zhang, X.; Loo, L. S. *Macromolecules* **2009**, *42*, 5196.

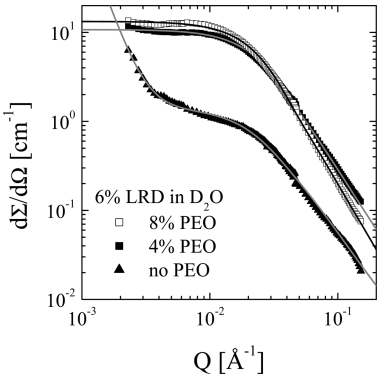

Figure 1. Static macroscopic cross section of 6% LRD in aqueous solutions with 0, 4, and 8% PEO. The solid lines describe model fits to the Beaucage function (eq 1) and also isolated clay particles with polymer decoration.

Neutron spin-echo (NSE) spectroscopy has the highest energy resolution in quasi-elastic neutron scattering and allows us to study the slow dynamics of mesoscopic objects such as thermally activated motions of polymer chains in solution.[15] The intermediate scattering function $S(q, \tau)$ measured with NSE, the Fourier transform of the scattering function $S(q, \omega)$, provides a means of investigating local effects of confinement of the polymer coils adsorbed at the surface of clay platelets. The neutron spin-echo experiments have been carried out at the J-NSE spectrometer[16,17] at the FRM II research reactor of TU München. A neutron wavelength of 8 Å has been used in the NSE experiments. The samples were placed into cells with quartz windows with a size of 30 × 30 mm^2, which matches the beam size on the J-NSE spectrometer. The path length was 2 mm. All experiments have been carried out at room temperature. Samples containing a mixture of clay and polymer have been background corrected with a sample containing clay only in D_2O. Additionally, a pure D_2O sample has been measured as background for the clay−D_2O sample in order to quantify the residual inelastic contributions from the clay and separate it from the polymer dynamics under investigation. The residual inelastic contributions result in corrections of less than 10%.

The macroscopic scattering cross sections for the 6 wt % Laponite gel without and with 4 and 8% polymer are shown in Figure 1. The scattering of the pure Laponite gel shows a Porod-like Q^{-4} scattering at small scattering angles ($Q < 0.003$ Å^{-1}) and scattering from independent particles, namely, the clay platelets, at scattering angles above 0.003 Å^{-1}. To describe the overall scattering, we used the following function (similar to that in ref 18):

$$\frac{d\Sigma}{d\Omega}(Q) = P_{Porod}Q^{-4} + G\left[\exp\left(-\frac{1}{3}Q^2R_g{}^2\right) + \frac{P}{\Gamma(P)}\left(\frac{QR_g}{\mathrm{erf}(1.06QR_g/\sqrt{6})^3}\right)^{-P}\right] \quad (1)$$

The first term arises from the large aggregates. Because of their large size, the Guinier behavior is not in the experimental window whereas the surface scattering is still observable as a Porod law. The Porod constant P_{Porod} describes the surface per volume of the large aggregates. The square bracket describes the scattering from isolated particles from the Guinier range to the fractal scattering at large scattering angles in the manner of Beaucage.[19] The forward scattering is given by G. The exponential term describes the Guinier behavior with R_g being the radius of gyration (i.e., the square root of the second moment of the mass distribution of particles). The residual term describes the fractal scattering of the particle with P being the fractal dimension. (Γ is the gamma function, and erf is the error function). The values of the fitting procedure are given in Table 1.

Table 1. Parameters Describing the Small-Angle Scattering of All Samples According to Equation 1

sample	6% LRD, 0% PEO	6% LRD, 4% PEO	6% LRD, 8% PEO
P_{Porod} (cm^{-1} Å^{-4})	(1.41 ± 0.01) × 10^{-10}	0, set	0, set
G (cm^{-1})	1.40 ± 0.015	10.78 ± 0.04	13.29 ± 0.06
R_g (Å)	70.8 ± 1.3	68.5 ± 0.6	71.9 ± 0.7
P	2, set	2.24 ± 0.03	2.46 ± 0.04

In parallel, the polymer-decorated clay particles can be described by the same function. Because the Porod behavior is only slightly indicated at the smallest Q, we simply set the contribution equal to zero. In a similar way, the background of these samples could be subtracted, and no fitting parameter was needed.

The discussion in the following text concentrates on the Guinier scattering of the isolated clay particles (decorated or not). It is compelling that the radius of gyration of the particles is constant and agrees with the producers' clay platelet diameter of 200 Å (thus $R_g = D/\sqrt{8} = 71$ Å whereas the thickness is $d = 10$ Å). In this sense, we argue that the scattering in the Q range from 0.003 to 0.2 Å^{-1} displays isolated clay particles that are decorated by polymer (if added). For the forward scattering of the isolated particles, we know in theory that

$$G = \frac{\phi_{clay}((\rho_{clay} - \rho_{D_2O})V_{clay} + (\rho_{polymer} - \rho_{D_2O})V_{polymer})^2}{V_{clay}} \quad (2)$$

The concentration ϕ_{clay} accounts for the volume fraction of isolated platelets. The scattering-length densities ρ_{clay}, $\rho_{polymer}$, and ρ_{D_2O} are 4.2×10^{-6}, -0.5×10^{-6}, and 6.5×10^{-6} Å^{-2}. The volume of one clay platelet is $V_{clay} = \pi dD^2/4 = 3.1 \times 10^5$ Å^3. The polymer volume arises from the total polymer attached to a single clay platelet. From the forward scattering of the pure clay sample, we obtain a volume fraction of 0.85% that is freely dispersed in the aqueous phase. This corresponds to the gel transition concentration of roughly 1%. In this sense, we have a saturated clay dispersion. A residue of roughly 5% forms large aggregates. In the following text, we would assume that the isolated clay fraction remains unchanged by the polymer. Then we can estimate the attached polymer following eq 2: For 4 and 8%, we find polymer volumes of 1.82×10^5 and 2.13×10^5 Å^3 corresponding to 5.5 and 6.5 polymers per clay platelet attached to the surface. In turn, this means that 0.50 and 0.58% are the volume fractions of polymer attached to the isolated clay platelets and 3.50 and 7.42% are the volume fractions of polymer in the aggregates (stacks). In the following text, we assume that the aggregates are formed by clay stacks with intercalated polymer. A high volume fraction of free polymer mainly opposes the dynamic measurements as discussed below. The physical argument for the low concentrations of free

(15) Richter, D.; Monkenbusch, M.; Arbe, A.; Colmenero, J. *Adv. Polym. Sci.* **2005**, *174*, 1–221.
(16) Monkenbusch, M.; Schätzler, R.; Richter, D. *Nucl. Instrum. Methods Phys. Res., Sect. A* **1997**, *399*, 301.
(17) Holderer, O.; Monkenbusch, M.; Borchert, G.; Breunig, C.; Zeitelhack, K. *Nucl. Instrum. Methods Phys. Res., Sect. A* **2008**, *586*, 90.
(18) Kammler, H. K.; Beaucage, G.; Mueller, R.; Pratsinis, S. E. *Langmuir* **2004**, *20*, 1915.
(19) Beaucage, G. *J. Appl. Crystallogr.* **1996**, *29*, 134.

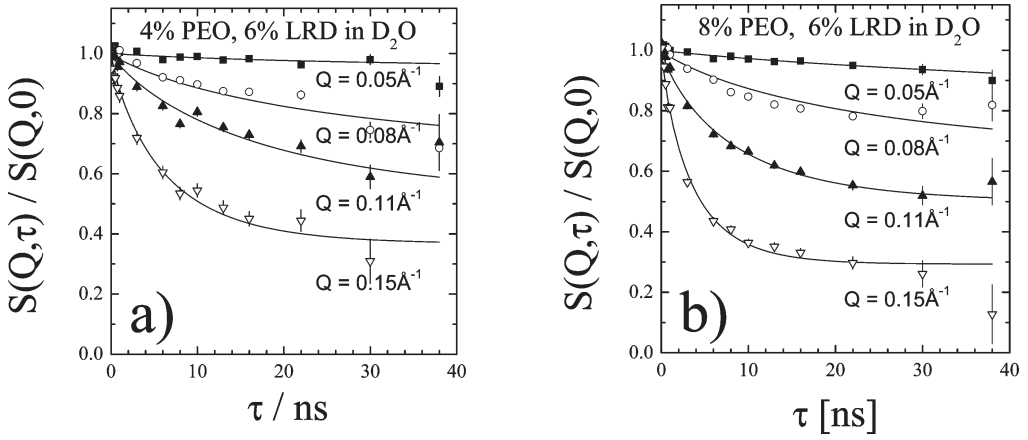

Figure 2. Intermediate scattering function of a clay dispersion with (a) 4 and (b) 8% polymer. The relaxation curves show plateau values dependent on the scattering vector Q. Solid lines are described by eq 3.

polymer in solution is that the intercalated state of the clay stacks entropically attracts the polymers more in comparison to the small water molecules. Another argument for slightly more polymer being bound to the isolated clay platelets arises from the fractal dimension of the scattering curves (being 2.24 and 2.46 for 4 and 8% polymer fractions). This shows that more polymer is attached for the 8% case and the surface looks more diffuse.

The intermediate scattering function $S(Q, t)/S(Q, 0)$ of the 4 and 8% samples is depicted in Figure 2. For NSE measurements, we purposely selected high $Q > 0.05$ Å^{-1}, where the fractal nature of the clay platelets appears ($Q^{-2.2}$ to $Q^{-2.5}$), so the attached polymer is studied as the decoration of a 2D object. Even at large scattering angles of $Q = 0.15$ Å^{-1} the scattering function is not fully relaxed at Fourier times of 30−40 ns. This observation motivated us to describe the scattering function as a sum of two modes,[12] one of which describes a free chain in solution (Zimm modes) and the other describing the tightly bound chains without motions on the considered timescale. The latter one means that neither the polymer fraction nor the clay particles relax in the considered time window. The application of Zimm theory to the current system is supported in the literature,[12] after it has been applied to polymer solutions.[21,22] For rather concentrated polymer gels, the Zimm theory was successfully applied.[12] The authors described the mobile fraction effectively by a stretched exponential as well. Furthermore, the concept of two fractions (mobile/immobile) had already been introduced. The immobile fraction describes the chain segments being rather tightly bound to the platelet, and the mobile fractions are the fractions of the polymer loops that are rather free. Throughout this article, we assume that there are no completely free chains (not attached to any clay platelet). The thus-obtained scattering function reads

$$\frac{S(Q,t)}{S(Q,0)} = (1-f_{(Q)})\exp(-(\Gamma_{(Q)}t)^{\beta}) + f_{(Q)} \qquad (3)$$

The Zimm[15,20] modes are described in a simplified manner by a stretched exponential function with a fixed exponent of $\beta = 0.85$. The relaxation rate Γ is assumed to be Q-dependent and therefore is fitted independently. In an ideal Zimm description, it depends on Q^3 according to $\Gamma = 0.253Q^3k_BT/\eta_S$,

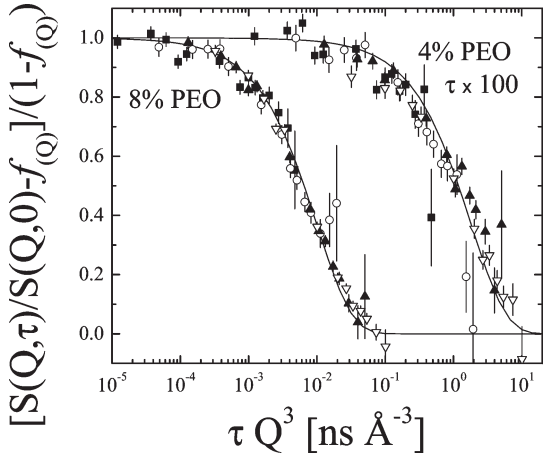

Figure 3. Zimm fraction of the intermediate scattering function as a function of the scaled time. The time axis of the 4% sample is multiplied by 100. For $Q = 0.05$, 0.11, and 0.15 Å^{-1}, the curves follow the simple Zimm scaling, but for $Q = 0.08$ Å^{-1}, the relaxation seems to take place at a different time.

with η_S being the solvent viscosity. The immobile fraction $f_{(Q)}$ is a fitting parameter as well.

The relaxing fraction of the polymer is plotted as a function of the Zimm-scaled time in Figure 3. Here it can be seen whether the assumed Zimm theory applies to this system. For scattering vectors $Q = 0.05$, 0.11, and 0.15 Å^{-1}, the Zimm scaling applies well. For $Q = 0.08$ Å^{-1}, we iteratively adjusted the immobile fraction $f_{(Q)}$ by ca. 6% to meet the scaling as seen in Figure 3. This adjustment is plausible within the obtained errors of the original fits to eq 3 because the uncertainty results mainly from the highest Fourier times τ (as seen in Figure 2). The individual fitting of eq 3 indicates a high sensitivity to each single data point. A physical model, as also described below, would still describe all data points with many fewer parameters. At this stage, we obtained a consistent description of the mobile fraction by the Zimm model.

The immobile fraction $f_{(Q)}$ of the polymer is plotted versus Q in Figure 4. Depending on the considered length scale, a certain amount of polymer appears to be attached to the clay particles. At large length scales, the whole polymer does not move with respect to the clay, whereas at smaller length scales movements of the polymer loops become visible. The interpretation is illustrated by the sketch in Figure 5. Such length-scale-dependent movements

(20) Ewen, B.; Richter, D. *Adv. Solid State Phys.* **1987**, *27*, 1.
(21) Nicholson, L. K.; Higgins, J. S.; Hayter, J. B. *Macromolecules* **1981**, *14*, 836.
(22) Richter, D.; Binder, K.; Ewen, B.; Stühn, B. *J. Phys. Chem.* **1984**, *88*, 6618.

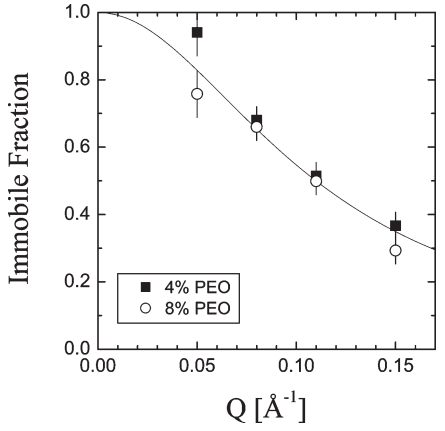

Figure 4. Immobile fraction as a function of the reciprocal scattering vector Q. The solid line describes the localization length. (See the text.)

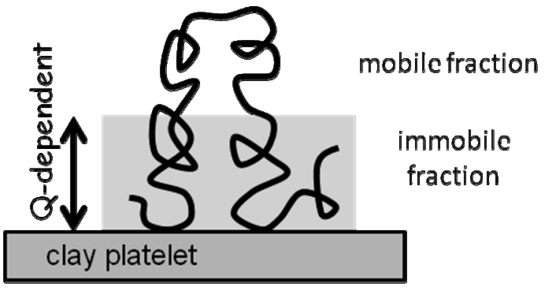

Figure 5. Sketch of an adsorbed polymer at a clay platelet. The immobile fraction near the solid surface is probed at high Q (and hence at short distances).

are often described by a Lorentz curve:[23]

$$f_{(Q)} = (1+\Xi^2 Q^2)^{-1} \quad (4)$$

The length Ξ can be interpreted as a localization length. For both polymer concentrations, we obtain the same length of 9 Å. From this, we would estimate the "sandwich" to have an overall thickness of ca. 28 Å (where both sides of the polymer covering do not cross talk). For the static SANS measurements, the polymer decoration appears to be a diffuse surface and therefore is not compact. This fact explains why the SANS measurements do not indicate a finite thickness of the overall sandwich. Only tedious contrast-variation measurements might finally unravel the static structure.

The relaxation rate Γ is depicted as a function of the cubed scattering angle Q^3 in Figure 6. As for Zimm motions, a linear dependence is expected. The relaxation rates agree quantitatively with the literature (Γ = 0.09−0.18 ns^{-1} at Q = 0.1 Å^{-1}).[12,13] From our relaxation rates, we would estimate the effective viscosities of the surroundings to $\eta_S = 0.253 Q^3 k_B T/\Gamma = 0.016$ and 0.0091 Pa s for the 4 and 8% samples. The higher polymer concentration leads to faster motions because the denser polymer is more rigid. This finding agrees qualitatively with the literature,[11] but not for pure gels.[12,13]

The dynamics can be described in more detail by the original models of polymers. For solutions, there is the Zimm[24] model,

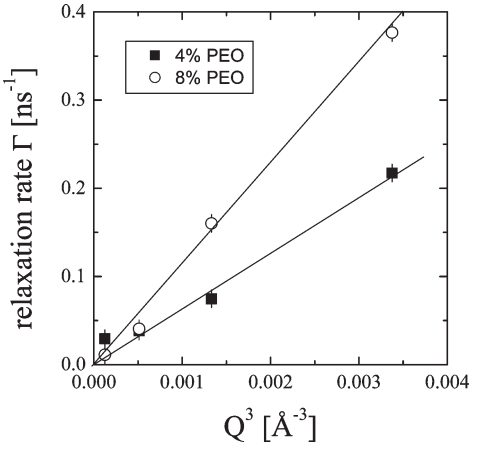

Figure 6. Dependence of the relaxation rate on the scattering vector Q for two different polymer concentrations. The higher polymer concentration leads to faster dynamics.

and for melts, there is the Rouse[25] model. These models can be extended by fixing single monomers inside a random coil and leaving the residual monomers free for fluctuations. For the Rouse model, the fixed monomers were chosen randomly and an ensemble average could be calculated.[25] The Zimm model treated the overall chain more regularly by fixing the middle monomer of N subchains of equal length. From the original modes described in ref 24, a regular pattern of residual modes was obtained and the relaxation of the confined polymer could be calculated. Unfortunately, this method remains undocumented in the literature. The compromise for both models at this stage is that the fixed points are placed inside the 3D coil instead of adjacent to a planar wall. The second step of improvement—inhibiting the penetration of the wall—is far from analytical treatments. For both models, we learn two things: The fixing of monomers inside the chain has huge effects. This condition makes clear why small changes in the number of polymers per clay particle (5.5 to 6.5) would lead to strong changes in the effective relaxation rate. For completeness, we mention a different approach that treats tethered chains as a homogeneous gel.[26]

This comparison leads us to the polymer brushes that were already described by DeGennes.[27,28] There are two modes (transverse and longitudinal): the single-fluid cooperative motion of the polymer with the solvent and a drag motion of the polymer with respect to the solvent. The first mode is faster than the latter. The fraction of the slow mode is 10.4% at the smallest Q and grows to 45% at the largest Q. Neither the tendency nor the absolute values resemble the immobile fraction of Figure 4. In this sense, the immobile fraction does not play the role of the longitudinal modes. We therefore assume that both contributions are seen as one total mobile fraction. The sum of both modes is described by an upside-down Lorentz function.[28] At present, we did not find a static contribution in the literature that would complete the picture in a manner suitable to our experimental findings.

In this article, we discussed the dynamics of surface-bound polymers. The single-sided confinement has a dramatic impact

(23) Pilippidi, E.; Michailidou, V.; Loppinet, B.; Rühe, J.; Fytas, G. *Langmuir* **2007**, *23*, 5139.
(24) Zimm, B. *J. Chem. Phys.* **1956**, *24*, 269.
(25) Niedzwiedz, K.; Wischnewski, A.; Monkenbusch, M.; Richter, D.; Genix, A. C.; Arbe, A.; Colmenero, J.; Strauch, M.; Straube, E. *Phys. Rev. Lett.* **2007**, *98*, 168301.
(26) Farago, B.; Monkenbusch, M.; Richter, D.; Huang, J. S.; Fetters, L. J.; Gast, A. P. *Phys. Rev. Lett.* **1993**, *71*, 1015.
(27) DeGennes, P. G. *Adv. Colloid Interface Sci.* **1987**, *27*, 189.
(28) Semenov, A. N.; Anastasiadis, S. H. *Macromolecules* **2000**, *33*, 613.

on the polymer motion. In our simple evaluation, the polymer could be described by two fractions: one immobile fraction bound to the clay and one mobile fraction with rather ideal dynamics of a chain in solution. The immobile fraction f is dependent on the scattering vector Q according to the highlighted spatial region. The localization length is directly connected to the polymer layer thickness and could be determined only by dynamic measurements in the given Q range. The higher polymer concentration leads to higher relaxation rates, which is typical of confined polymers.